The TOKAM3X code for edge turbulent fluid simulation for tokamak plasma in versatile magnetic geometries

E. Serre[1]

H. Bufferand[1,2], G. Ciraolo[1,2], C. Colin[1], D. Galassi[1], Ph. Ghendrih[2], Y. Marandet [3], F. Schwander[1], P. Tamain[2]

[1]Aix Marseille Université-CNRS-Centrale Marseille, M2P2, Marseille, France
[2]CEA, IRFM, France
[3]PIIM, Aix Marseille Université-CNRS

Journées IPL Fratres, Sophia-Antipolis 15/10/2015

The tokamak: an out-equilibrium thermodynamic device

- For fusion operation: two critical issues $\rightarrow$ quality of plasma confinement + heat exhaust both involve turbulent transport
- ITER will require predictive numerical simulations
- Call for a modelling effort
- TOKAM3X + SOLEDGE2D-EIRENE is part of this effort started 10 years ago between CEA and Aix-Marseille

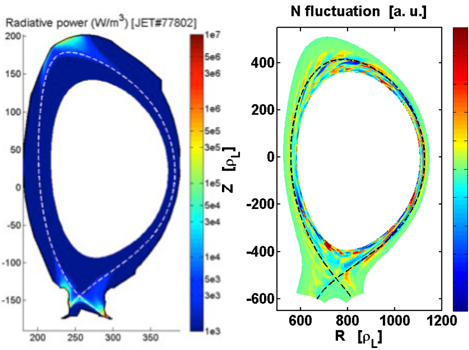

Figure: From 2D transport to 3D turbulence simulations in a JET-like geometry. SOLEDG2D-EIRENE neutral radiations (left) and TOKAM3X density fluctuations (right)

THE EDGE / SOL PLASMA

In tokamak, the plasma is confined within the Last Closed Flux Surface. A scrape-off layer (SOL) is generated at the boundary where ionized impurities flow along field lines into the divertor.

THE OUTER TOKAMAK REGION

- External core plasma + Scrape off layer (SOL)
- Up to the plasma facing components (PFC)

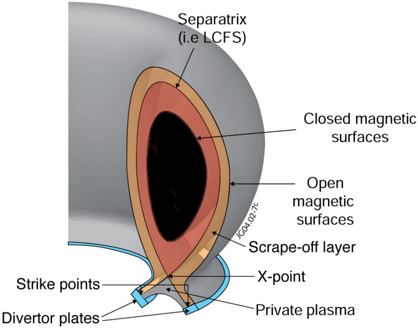

- Various complexity mimicking most of the actual tokamaks
- A fixed cyl. (R, Z, φ) + a curvilinear system of coordinates $(\psi, \widehat{\theta}, \varphi)$
- A magnetic field $\vec{B} = B\vec{b}$
  $\vec{B} = F\vec{\nabla}\varphi + \vec{\nabla}\Psi \times \vec{\nabla}\varphi$
  F: toroidal flux number $\Psi(R, Z)$: poloidal flux function (prescribed)

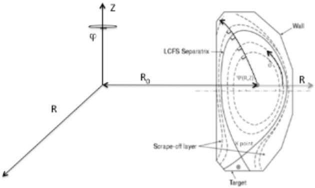

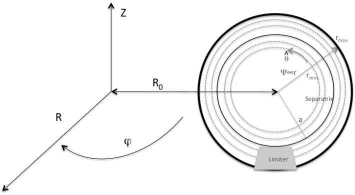

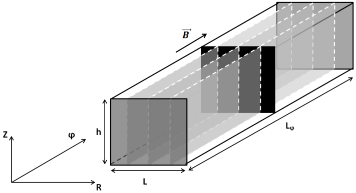

3D DRIFT-REDUCED TWO-FLUID EQUATIONS

5 MAIN ASSUMPTIONS

1. $\rho_L \gg \lambda_D \Rightarrow$ **electroneutrality** $(n_e \simeq Zn_i)$ + no sheath (appears thanks to Bohm bc)
2. **Negligeable electron inertia**, $m_e/m_i \simeq O(10^{-3}) \Longrightarrow m_e << m_i$,
3. **Drift ordering**: $\epsilon_\omega = \omega/\omega_{ci} \ll 1 \Rightarrow$ a strong scale separation $\rho_L(\simeq 1mm) << l_t(\simeq 0.1 - 10cm)$
   Useful to split the dynamics into the $\|$ and $\perp$ direction to B:
   $$\vec{u}^{i,e} = u_{\|}^{i,e}\vec{b} + \vec{u}_{\perp}^{i,e}$$
   $\perp$ *components are expicitly known in terms of drifts*:
   $$\vec{u}_{\perp}^{i} = \vec{u}_E + \vec{u}_{\nabla B}^{i} + \vec{u}_p^{i} \text{ and } \vec{u}_{\perp}^{e} = \vec{u}_E + \vec{u}_{\nabla B}^{e}$$
4. $nT/(B^2/2\mu_0) \ll 1 \Rightarrow$ **electrostatic plasma**
5. **Isothermal** $T_i = T_e = T_0$

3D drift-reduced two-fluid equations

Continuity

$$\partial_t N + \vec{\nabla} \cdot \left(N \vec{u^e} \right) = S_N + \vec{\nabla} \cdot \left(D_N \vec{\nabla_\perp} N \right) \quad (1)$$

Ion parallel momentum conservation

$$\partial_t \Gamma + \vec{\nabla} \cdot \left(\Gamma \vec{u^i} \right) = -\nabla_\parallel P + \vec{\nabla} \cdot \left(D_\Gamma \vec{\nabla_\perp} \Gamma \right) \quad (2)$$

Electron momentum conservation through generalized Ohm law

$$\eta_\parallel N j_\parallel = -N \nabla_\parallel \phi + \nabla_\parallel N \quad (3)$$

Charge conservation

$$\nabla . \vec{j} = 0 \quad (4)$$

with $D_{N,\Gamma}$ effective diffusions, S_N a source term driving the particle flux, P the pressure $P = P_e + P_i = N(T_i + T_e) = 2N$.

with also

$$\vec{j} = j_{\parallel}\vec{b} + \vec{j_{\nabla B}} + \vec{j_p} \tag{5}$$

$$\Longleftrightarrow \vec{j} = j_{\parallel}\vec{b} + Ne(\vec{u}^i_{\nabla B} - \vec{u}^e_{\nabla B}) + Ne\vec{u}^i_p, \tag{6}$$

The charge balance equation (4) (+ Boussinesq approx) leads to:

Vorticity equation

$$\partial_t W + \vec{\nabla}\cdot(W\vec{u}^i) = \vec{\nabla}\cdot\left(N(\vec{u}^i_{\nabla B} - \vec{u}^e_{\nabla B}) + j_{\parallel}\vec{b}\right) + \vec{\nabla}\cdot(D_W\vec{\nabla}_{\perp}W) \tag{7}$$

with $W = \vec{\nabla}\cdot\left(\frac{1}{B^2}\left(\vec{\nabla}_{\perp}\phi + \vec{\nabla}_{\perp}P_i\right)\right)$

Boundary conditions

Parallel direction in the SOL: sheath transmission

- Bohm : $|u_{\|}/c_s| \geq 1 \Longleftrightarrow |\Gamma| \geq N$
- $J_{\|} = \pm N c_s \left(1 - exp(\Lambda - \phi)\right) \simeq \pm N(\Lambda - \phi)$
  Λ the sheath floating potential

  $+$ Ohm law $\rightarrow$ parallel derivative of the potential
  $\nabla_{\|}\Phi = \pm \eta_{\|} N(\Lambda - \phi) + \frac{\nabla_{\|} N}{N}$

Perpendicular direction in the SOL and core

- $\partial_{\perp}(.) = 0$

- Mapped any domain into a set of rectangular subdomains
  $\rightarrow$ To keep a structured flux-surfaces aligned mesh whatever the geometry
  $\rightarrow$ Efficient for parallelization
- Ghosts cells store the information on the neighbourhood within a matrix that defines how these domains are connected to each other.

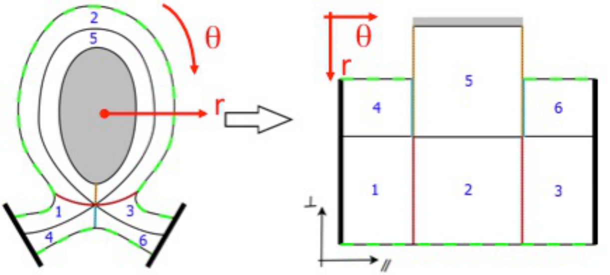

Example of domain decomposition in 6 subdomains of a diverted geometry

The numerics: the grid

- A structured magnetic flux-surface aligned grid
- In each subdomain: grid points indexed by $(i_\psi, i_{\hat{\theta}}, i_\varphi)$, for $i_\psi = 1, \ldots N_\psi$, $i_{\hat{\theta}} = 1, \ldots N_{\hat{\theta}}$, $i_\varphi = 1, \ldots N_\varphi$ and defined by their special coordinates (R, Z, φ).
- Differential operators evaluated using metric coefficients

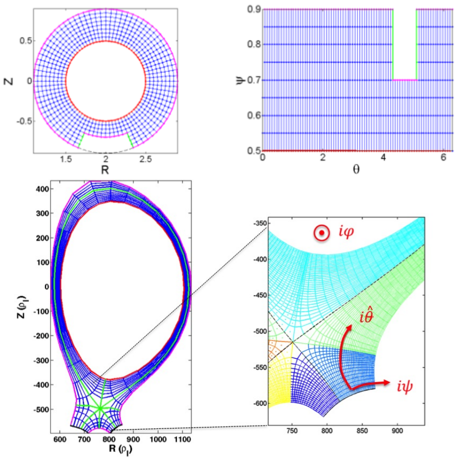

Examples of meshes in limited circular (top) and diverted (botto) poloidal cross-sections.

The numerics: the discretization

- A second-order conservative finite-differences scheme associated to a 3rd-order WENO reconstruction for the advection terms
- A first-order Implicit - explicit splitting scheme for time discretization (a Runge-Kutta of arbitrary order is now implemented)
- Hybrid MPI + OpenMP parallelization data exchange typical cases = 100-200 processes $\simeq 60\%$ efficiency

Advection and source terms

$$\begin{aligned}
\partial_t N &= \ldots - \vec{\nabla}\cdot(\Gamma\vec{b}) - \vec{\nabla}\cdot(N\vec{u}_E) - \vec{\nabla}\cdot(N\vec{u}^e_{\nabla B}) + S_N \\
\partial_t \Gamma &= \ldots - \vec{\nabla}\cdot(\frac{\Gamma^2}{N}\vec{b}) - \vec{\nabla}\cdot(\Gamma\vec{u}_E) - \vec{\nabla}\cdot(\Gamma\vec{u}^i_{\nabla B}) - 2\nabla_{\parallel}N + S_\Gamma \\
\partial_t W &= \ldots - \vec{\nabla}\cdot(\frac{W\Gamma}{N}\vec{b}) - \vec{\nabla}\cdot(W\vec{u}_E) - \vec{\nabla}\cdot(W\vec{u}^i_{\nabla B}) \\
&+ \vec{\nabla}\cdot(N(\vec{u}^i_{\nabla B} - \vec{u}^i_{\nabla B}))
\end{aligned} \tag{8}$$

- $\|$ and $\perp$ advection
- Mainly non-linear
- Dynamics over ionic time scale
  $\rightarrow$ explicit advancement

Parallel current terms

$$
\begin{aligned}
\partial_t W &= ... + \vec{\nabla} \cdot (j_{\|} \vec{b}) \\
W &= \vec{\nabla} \cdot \left(\frac{1}{B^2} (\vec{\nabla}_{\perp} \phi + \vec{\nabla}_{\perp} N) \right) \\
j_{\|} &= \frac{1}{\eta_{\|}} \left(\frac{\nabla_{\|} N}{N} - \nabla_{\|} \phi \right)
\end{aligned} \tag{9}
$$

- Evolution of the plasma electric potential Φ
- Associated to fast dynamics
  $\rightarrow$ implicit advancement
- Inversion of a badly conditionned 3D operator

Perpendicular diffusion terms

$$
\begin{aligned}
\partial_t N &= ... + \vec{\nabla}_\perp \cdot \left(D_N \vec{\nabla}_\perp N \right) \\
\partial_t \Gamma &= ... + \vec{\nabla}_\perp \cdot \left(D_\Gamma \vec{\nabla}_\perp \Gamma \right) \\
\partial_t W &= ... + \vec{\nabla}_\perp \cdot \left(D_W \vec{\nabla}_\perp W \right)
\end{aligned}
$$

- Evolution of the plasma electric potential Φ
- Associated to fast dynamics
  $\rightarrow$ implicit advancement
- Inversion of a badly conditionned 3D operator

These terms are advanced implicitly in order to allow large diffusion coefficient, running the code in transport mode (i.e. no turbulent small scales).

1. Explicit advancement of advection and source terms

$$\begin{bmatrix} N^\star \\ \Gamma^\star \\ W^\star \end{bmatrix} = \begin{bmatrix} N^{n-1} \\ \Gamma^{n-1} \\ W^{n-1} \end{bmatrix} + \delta t \begin{bmatrix} \mathcal{F}_N\left(N^{n-1}, \Gamma^{n-1}, W^{n-1}\right) \\ \mathcal{F}_\Gamma\left(N^{n-1}, \Gamma^{n-1}, W^{n-1}\right) \\ \mathcal{F}_W\left(N^{n-1}, \Gamma^{n-1}, W^{n-1}\right) \end{bmatrix} + \delta t \begin{bmatrix} S_N \\ S_\Gamma \\ S_W \end{bmatrix}$$

where $\mathcal{F}_{N,\Gamma,W}$ are decomposed as follow:

$$\begin{bmatrix} \mathcal{F}_N\left(N^{n-1}, \Gamma^{n-1}, W^{n-1}\right) \\ \mathcal{F}_\Gamma\left(N^{n-1}, \Gamma^{n-1}, W^{n-1}\right) \\ \mathcal{F}_W\left(N^{n-1}, \Gamma^{n-1}, W^{n-1}\right) \end{bmatrix} = \begin{bmatrix} \mathcal{F}_N^{||}\left(N^{n-1}, \Gamma^{n-1}\right) \\ \mathcal{F}_\Gamma^{||}\left(N^{n-1}, \Gamma^{n-1}\right) \\ 0 \end{bmatrix} +$$

$$\begin{bmatrix} 0 \\ 0 \\ \mathcal{F}_W^{||}\left(N^{n-1}, \Gamma^{n-1}, W^{n-1}\right) \end{bmatrix} + \begin{bmatrix} \mathcal{F}_N^{\perp}\left(N^{n-1}, \Gamma^{n-1}, W^{n-1}\right) \\ \mathcal{F}_\Gamma^{\perp}\left(N^{n-1}, \Gamma^{n-1}, W^{n-1}\right) \\ \mathcal{F}_W^{\perp}\left(N^{n-1}, \Gamma^{n-1}, W^{n-1}\right) \end{bmatrix}$$

$\mathcal{F}^{||}_{N,\Gamma,W}$ and $\mathcal{F}^{\perp}_{N,\Gamma,W}$: explicit fluxes (WENO).

$\mathcal{F}^{||}_{N,\Gamma,W}$: compressible dyn. require the (N, Γ) coupling (Riemann solver).

$\mathcal{F}^{\perp}_{N,\Gamma,W}$: passive scalars advection by prescribed drift.

2. Implicit advancement of parallel current terms Main numerical issue associated to an extremely fast dynamics. Time evolution of Φ such that:

$$\left(\mathcal{L}^{\perp} + \ \delta t \ \mathcal{L}^{\parallel}\right)\phi^{\star\star} = W^{\star} - \mathcal{L}^{\perp} N^{\star} + \ \delta t \ \mathcal{L}^{\parallel} lnN^{\star} \tag{10}$$

where $\mathcal{L}^{\perp,\parallel}$ are spatial differential operators: $\mathcal{L}^{\perp} = \vec{\nabla} \cdot \left(\frac{1}{B^2}\vec{\nabla}_{\perp}\cdot\right)$ and $\mathcal{L}^{\parallel} = \vec{\nabla} \cdot \left(\frac{1}{\eta_{\parallel}}\vec{b}\nabla_{\parallel}\cdot\right)$

- 3 coupled directions $\rightarrow$ inversion of a $3D$ operator.
- Small values of $\eta_{\parallel}$ $\rightarrow$ very badly conditionned operator hindering up to now the use of an efficient iterative scheme.
- LU decomposition thanks to the PASTIX library.

3. Implicit advancement of perpendicular diffusion terms

$$\begin{bmatrix} \left(1-\delta t\ \mathcal{D}_N^{\perp}\right)\ N^n \\ \left(1-\delta t\ \mathcal{D}_\Gamma^{\perp}\right)\ \Gamma^n \\ \left(1-\delta t\ \mathcal{D}_W^{\perp}\right)\ W^n \end{bmatrix} = \begin{bmatrix} N^\star \\ \Gamma^\star \\ W^\star \end{bmatrix} \tag{11}$$

where $\mathcal{D}_{N,\Gamma,W}^{\perp} = \vec{\nabla}_\perp \cdot \left(D_{N,\Gamma,W}^{\perp}\vec{\nabla}_\perp \cdot\right)$.

$\mathcal{D}_{N,\Gamma,W}^{\perp}$ constant and do not depend on φ
$\rightarrow N_\varphi$ 2D matrices (one for each toroidal positions) which are stored during preprocessing.

Steady manufactured solution

- Circular cross section ($\psi = r$, $\hat{\theta} = r\theta$) + closed field lines (no limiter)
- Smooth and easily handable solutions for calculations:

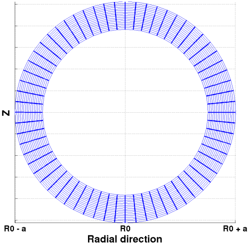

$$\begin{cases} N_{ana} = (1+\beta cos(2\pi t))(N_0 + sin(\frac{2\pi r}{a}) sin(\theta) cos(\varphi)) \\ \Gamma_{ana} = (1+\beta cos(2\pi t)) sin(\frac{2\pi r}{a}) sin(\theta) cos(\varphi) \\ \Phi_{ana} = (1+\beta cos(2\pi t)) sin(\frac{2\pi r}{a}) sin(\theta) cos(\varphi) \end{cases}$$

$(\theta, \varphi) \in [0, 2\pi]$ and $r \in [a, r_{max}]$. $\beta = 1$ or 0, depending on the analytical solution is time-dependent or not

Convergence results

L_2 discrete norm for N, Γ and W and for 5 grids

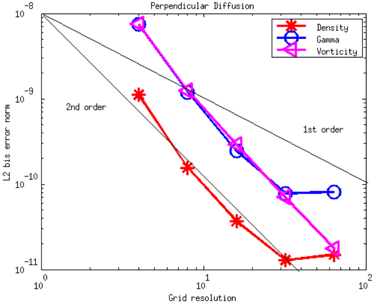

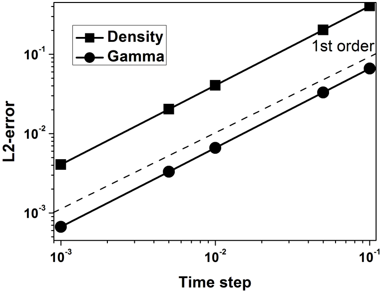

$$L_2(F) = \left(\frac{1}{N_r N_\theta N_\varphi} \sum_{ijk} |F_{ijk} - F_{ijk}^{ana}|^2 \right)^{1/2} \quad (12)$$

Simulations in slab geometry

- Space and time evolution of a localized surdensity over a plasma equilibrium
- Overall agreement with TORPEX measurements (Theiler *et al.* PRL 09): the blob starts faster but slows down later

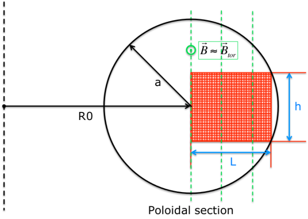

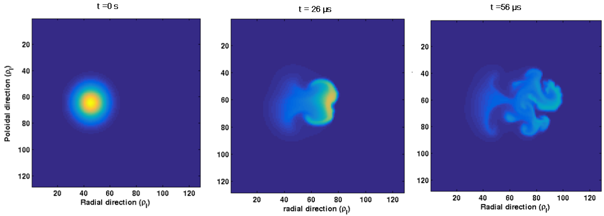

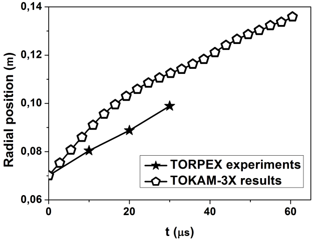

A classic mushroom shape related to a Rayleigh-Bénard instability mechanism

Code validation: MISTRAL test case

- Moving the plasma contact point on Tore-Supra (Dif-Pradalier *et al.* JNM11): new evidence of asymmetry around the outboard mid-plane
- Demanding test bench: mimic by changing the limiter location
- Same trends than in experiments (details in Colin *et al.* 2014): iso-lines $M_{\|} = 0$ not symmetric / the limiter position

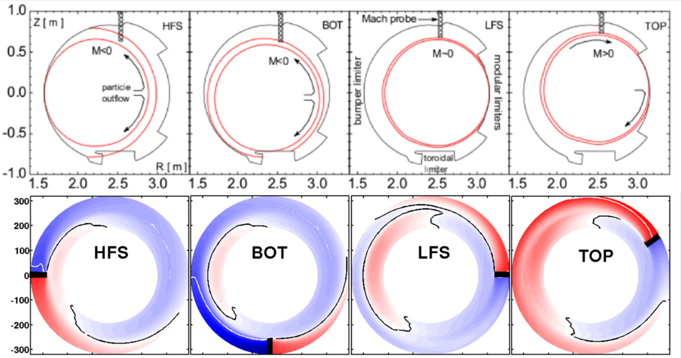

Gunn et al. JNM 07; Averaged $M_{\|}$ TOKAM3X grid: $64 \times 256 \times 64$ in (r, θ, φ). $\delta t = 2$

Simulations: set-up

Interchange turbulence in a diverted plasma

- Mechanism: B curvature: $\gamma^2 \propto \nabla B \cdot \nabla N$ (Rayleigh-Benard)
- Exists on the LFS, $\partial_r(\frac{1}{B}) > 0$

Numerical set-up

- JET like poloidal cross section
- Computational domain: $a = 256\rho_L$ (lower than in JET)
- Parameters: $D_{N,\Gamma,W} = 10^{-2}\rho_L^2\omega_c$, $\eta_{\|} = 10^{-5}$
- Typical grids: $32 \times 512 \times 128$ (core), $32 \times 544 \times 128$ (SOL and divertor) and $16 \times 16 \times 128$ (private flux region) in (r, θ, φ).
- Dimensionless time-step $\delta t = 1$.
- Computations run on the Aix-Marseille University computing center using 144 cores (120h CPU).

Simulations: results

- Far from the X-point, similar behaviour than in limiter geometry (Tamain *et al.* CPP14)
  → Large poloidal asymmetries that correspond to a ballooned turbulence around the Low Field Side mid-plane.
  → Changes across the separatrix: from quasi null skewness ($r < a$) to positive one ($r > a$)

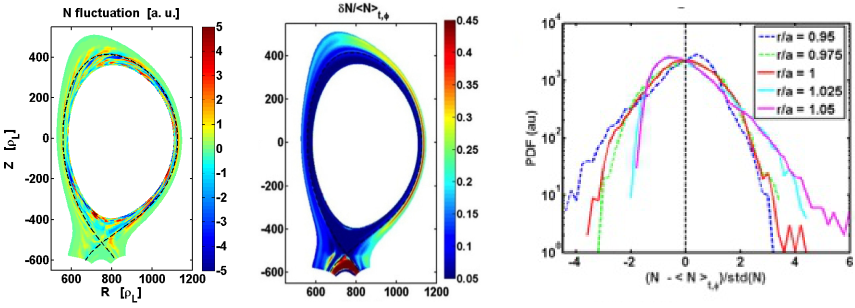

Density fluctuations (left) and standard deviation normalized by the mean density (middle) in the poloidal plane showing interchange turbulence in a diverted plasma.(right) PDF at LFS midplane across the separatrix.

- This is also supported by the time evolution of the density recorded at seven poloidal locations

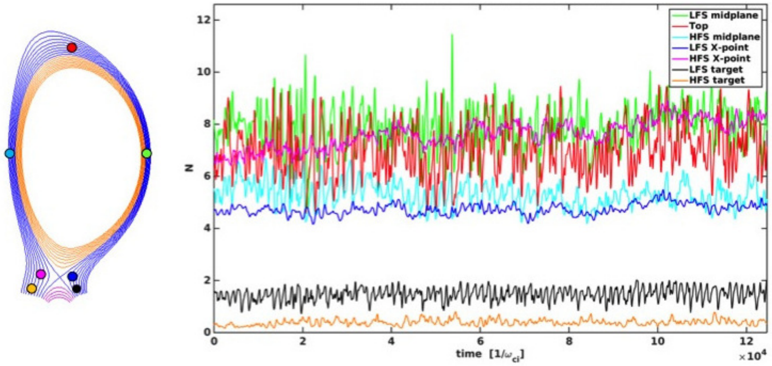

Time evolution of the density N recorded at seven different positions in the poloidal plane.

Simulations: results

- However, on contrary to limited simulations the X-point leads to a steep topological discontinuity
- Specific physics at play to investigate.
- Divertor acts as a big plasma sink: large poloidal gradients $\rightarrow$ complex $E \times B$ velocity and parallel flow pattern in its vicinity.

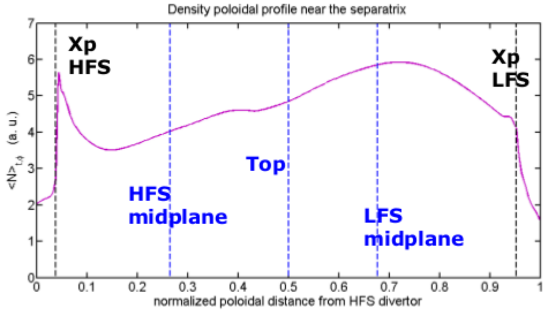

Time evolution of the density N recorded at seven different positions in the poloidal plane.

Concluding remarks

TOKAM3X workplan

- Improvement of the vorticity operator inversion
  $\rightarrow$ Find an efficient preconditionners?
  $\rightarrow$ AP scheme?
  $\rightarrow$ Evaluation of an explicit solver
- Use field aligned interpolation (talk M. Mehrenberger)
- Implementation of an immersed boundary technique
- TOKAM3X-EIRENE coupling